

Creation of highly stable monomeric Pd(II) species in an anion-exchangeable hydroxy double salt interlayer: Application to aerobic alcohol oxidation under an air atmosphere†

Takayoshi Hara, Masakazu Ishikawa, Junya Sawada, Nobuyuki Ichikuni and Shogo Shimazu*

Received 26th June 2009, Accepted 4th September 2009

First published as an Advance Article on the web 23rd October 2009

DOI: 10.1039/b918350g

An active Pd(II) catalyst supported on the Ni–Zn mixed basic salt (NiZn), which is classified by the anion-exchangeable layered hydroxy double salts, was synthesized by simple intercalation of the anionic Pd(II) hydroxyl complex. The divalent Pd species in the interlayer of NiZn maintained their original monomeric structure during the aerobic alcohol oxidation, due to the strong electrostatic interaction between the NiZn host and anionic Pd(II) species. This catalyst could be reused without any loss of the catalytic activity and selectivity in the aerobic alcohol oxidation.

Introduction

In order to achieve environmentally benign oxidation reactions, precise control of the local structure of the catalytically active species is required. A number of groups have recently reported relevant examples.¹ In the case of aerobic alcohol oxidation using transition metal-based heterogeneous catalysts,² supported Pd nanoparticles often exhibit highly efficient reactions.³ In order to achieve green organic syntheses of high-value chemicals including asymmetric molecules,⁴ the use of functional materials as catalyst supports abates the need for organic ligands often required to stabilize monomeric Pd species.⁵

Hydroxy double salts (HDSs) and layered double hydroxides (LDHs) have received considerable interest as anion-exchangeable layered compounds due to their potential applications as catalyst supports.⁶ The Ni–Zn mixed basic salt (NiZn), classified as a type of HDS, has a typical chemical composition of $\text{Ni}_{1-x}\text{Zn}_x(\text{OAc})_{2x}(\text{OH})_2 \cdot n\text{H}_2\text{O}$ ($0.15 < x < 0.25$).⁷ The structure of NiZn, where at most one quarter of the octahedral Ni sites in the $\text{Ni}(\text{OH})_2$ layer are vacant and where the divalent tetrahedral Zn cations are coordinated and stabilized just below and above the empty Ni sites, facilitates the formation of an excess positive layer charge, as illustrated in Fig. 1.

The choice of NiZn as a catalyst support is motivated by the following advantages: (i) simple preparation, (ii) high crystallinity, (iii) strongly isolated anion-exchangeable sites and neighboring Zn^{2+} cations, and (iv) strong electrostatic interactions between guest anions and Zn^{2+} cations. Since good catalysts are expected to show high selectivity and high stability, inorganic supports are required to have high dimensional structures which have a linker site as well as a reaction auxiliary site.

Here, we present a new strategy for the design of a novel green aerobic alcohol oxidation catalyst based on the unique

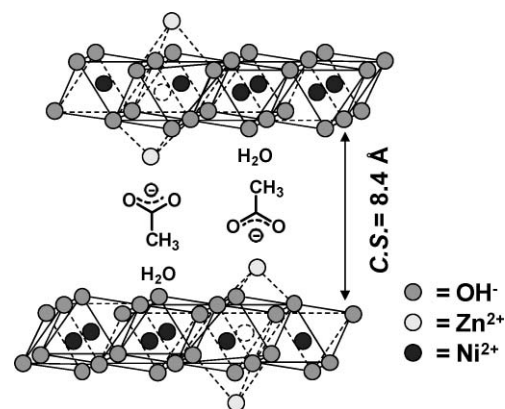


Fig. 1 Schematic structure of Ni–Zn mixed basic salt (NiZn).

characteristics of NiZn. In our catalyst system, the fixed monomeric divalent Pd species as an active site in a NiZn interlayer are inhibited from aggregating into unreactive Pd metal due to strong electrostatic interactions, thereby removing the need for organic stabilizers. To clarify the special features of NiZn, hydrotalcite (HT), $\text{Mg}_6\text{Al}_2(\text{OH})_{16}(\text{CO}_3) \cdot 4\text{H}_2\text{O}$, as a general anion-exchangeable clay was also used as a catalyst support.

Results and discussions

The strategy of our work is the intercalation of an anionic $[\text{Pd}(\text{OH})_4]^{2-}$ species into an interlayer of NiZn. It is reported that this anionic species was able to be prepared by the hydrolysis of palladium chloride in water: K_2PdCl_4 was treated with an aqueous solution of NaOH (0.1 M).⁸ In the UV-vis spectra, the Pd–Cl charge transfer band around 234 nm disappeared after treatment with alkaline water (Fig. 2b). In the Fourier transforms (FT) of k^3 -weighted Pd K-edge EXAFS spectra, the peak around 1.9 Å corresponding to the Pd–Cl bond also disappeared, and the peak around 1.5 Å originating from the formation of the Pd–O bond was observed without the peaks

Department of Applied Chemistry and Biotechnology, Graduate School of Engineering, Chiba University, 1-33, Yayoi-cho, Inage-ku, Chiba, 263-8522. E-mail: shimazu@faculty.chiba-u.jp; Fax: +81-43-290-3379

† Electronic supplementary information (ESI) available: Experimental details. See DOI: 10.1039/b918350g

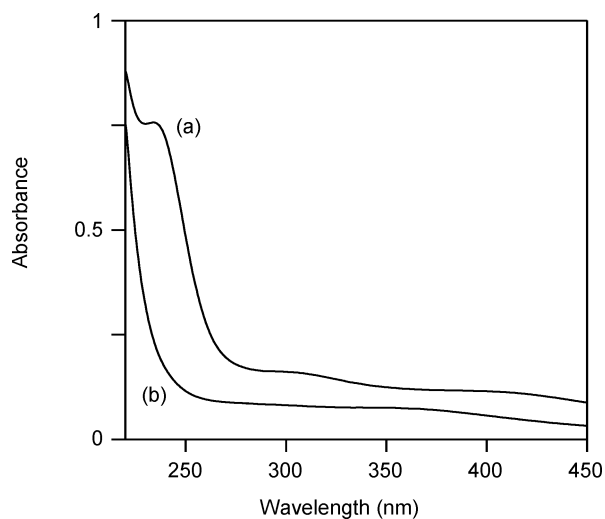


Fig. 2 UV-vis spectra for (a) aqueous K_2PdCl_4 solution and (b) aqueous K_2PdCl_4 solution treated with NaOH.

detected in the Pd foil or the Pd oxide at 2.5 and 3.0 Å corresponding to Pd–Pd and Pd–O–Pd bonds (Fig. 3). The peak around 1.5 Å in Fig. 3b was well fitted by use of the Pd–O shell parameter and four oxygen atoms at 2.01 Å confirmed by the curve-fitting analysis (Table 1). This result means that the $[\text{Pd}(\text{OH})_4]^{2-}$ species was formed in aqueous solution.

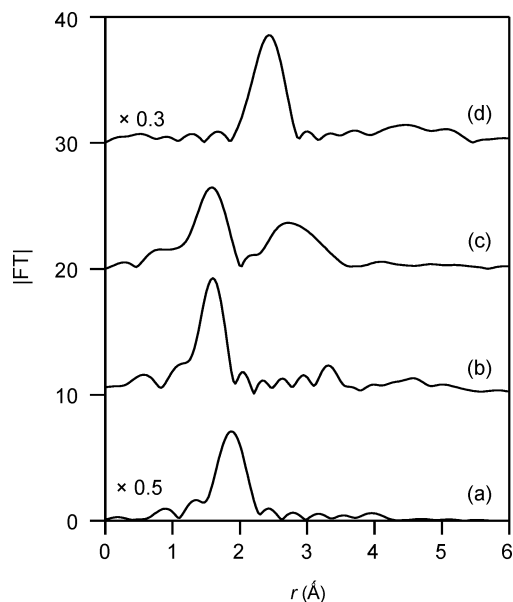


Fig. 3 FT of k^3 -weighted Pd K-edge EXAFS for (a) K_2PdCl_4 , (b) aqueous solution of K_2PdCl_4 with NaOH, (c) Pd oxide and (d) Pd foil.

The NiZn was synthesized by a previously reported procedure.^{7a} Based on characterization by XRF, and TG-DTA, the chemical formula and anion-exchange capacity of NiZn were found to be $\text{Ni}_{0.78}\text{Zn}_{0.44}(\text{OAc})_{0.44}(\text{OH})_2 \cdot 0.86\text{H}_2\text{O}$ (Ni/Zn = 1.77) and 2.65 mmol g^{-1} , respectively. Immobilization of the palladium precursor in the NiZn interlayer was achieved by the anion-exchange method. Treatment of NiZn with $[\text{Pd}(\text{OH})_4]^{2-}$ yielded the NiZn-intercalated Pd(II) hydroxyl complex, Pd/NiZn(0.02) and Pd/NiZn(1) as a green powder (number in parenthesis indicates Pd loading amount in a unit of mmol g^{-1}). The

Table 1 Curve-fitting analysis for the preparation solution^a

Sample	Shell	C.N. ^b	r (Å) ^c	σ (Å) ^d
K_2PdCl_4 with NaOH aq.	Pd–O	4.0	2.01	0.044
	$\text{K}_2\text{PdCl}_4^e$	Pd–Cl	4	2.32
	Pd oxide ^e	Pd–O	4	2.02
		Pd–O–Pd (1)	4	3.03
Pd foil ^e	Pd–O–Pd (2)	8	3.42	
	Pd–Pd	12	2.74	

^a Curve-fitting analysis was performed with the inverse FT of the $0.95 \text{ \AA} < r < 2.03 \text{ \AA}$ range using PdO as a standard material. ^b Coordination number. ^c Bond distance. ^d Debye–Waller factor. ^e Data from X-ray crystallography.

Pd/HT(0.02) catalyst was prepared in the same manner, using HT instead of NiZn. XRD profiles revealed that Pd/NiZn(0.02) and the parent NiZn had the same layered structures, and the clearance space (C. S.), calculated from the d_{001} peak, was 8.4 Å (Fig. 4a and 4b). In contrast, the C. S. of NiZn narrowed to 4.4 Å after intercalation of a high Pd content (1 mmol g^{-1} , Fig. 4c), due to the anion exchange of acetate for the hydroxyl anion.⁹ In the case of the HT supports, the C. S. of Pd/HT(0.02) maintained a similar distance of the parent HT (7.9 Å).

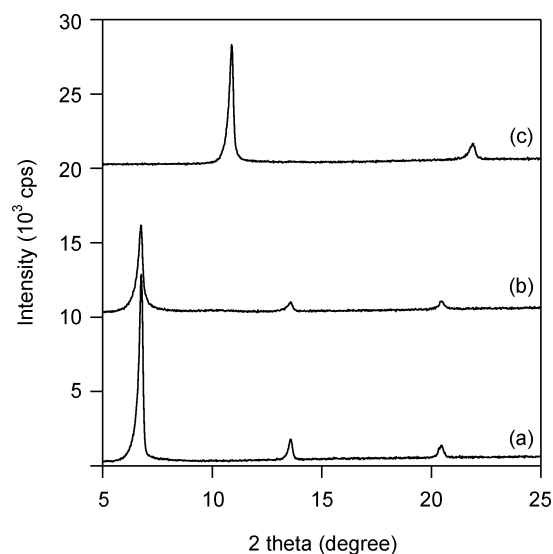


Fig. 4 XRD profiles for (a) NiZn, (b) fresh Pd/NiZn(0.02) and (c) fresh Pd/NiZn(1).

To determine the local structure of the various Pd–clay nanocomposite catalyst, XAFS analyses were carried out. The features of the Pd K-edge XANES spectrum (Fig. 5) and the edge energy of fresh Pd/NiZn(0.02), fresh Pd/HT(0.02), and fresh Pd/NiZn(1) did not resemble those of Pd foil but were similar to those of Pd oxide. This similarity suggests that divalent Pd species are present in all of the clays. The FT of the k^3 -weighted EXAFS data are shown in Fig. 6. In the second coordination sphere of fresh Pd/NiZn(0.02), fresh Pd/HT(0.02), and Pd/NiZn(1), the peaks observed in the Pd foil or the Pd oxide corresponding to Pd–Pd and Pd–O–Pd bonds were not observed. The inverse FT of the peaks in the range of 1–2 Å for the fresh Pd–clay nanocomposite catalysts corresponded to oxygen atoms (Table 2). In the case of fresh Pd/NiZn(0.02), four oxygen atoms at 2.01 Å were observed

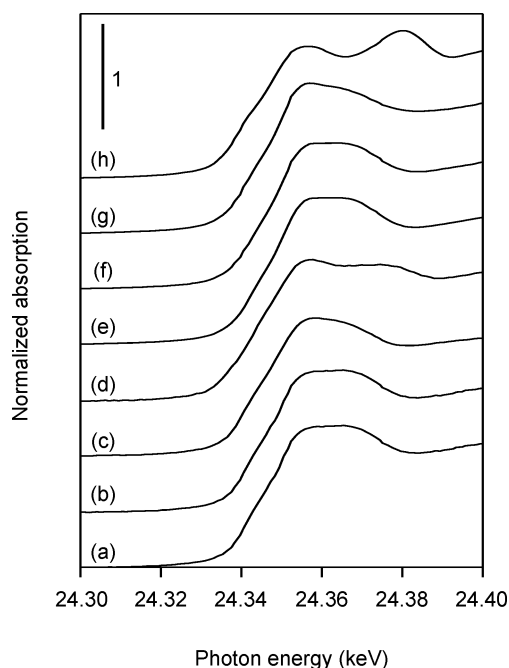


Fig. 5 Pd K-edge XANES spectra for (a) fresh Pd/NiZn(0.02), (b) recovered Pd/NiZn(0.02), (c) fresh Pd/HT(0.02), (d) recovered Pd/HT(0.02), (e) fresh Pd/NiZn(1), (f) recovered Pd/NiZn(1), (g) Pd oxide and (h) Pd foil.

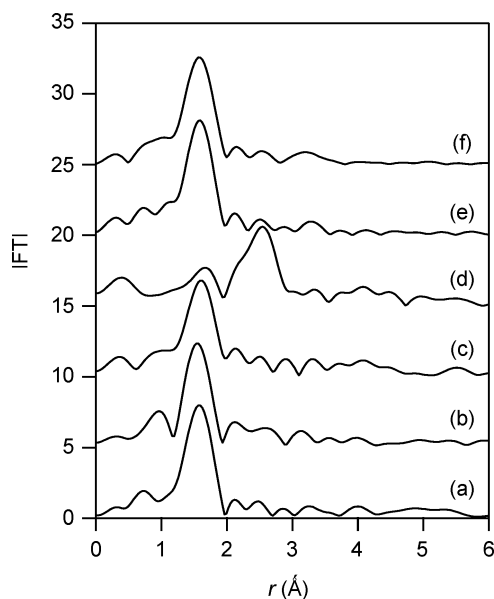


Fig. 6 FT of k^3 -weighted Pd K-edge EXAFS for (a) fresh Pd/NiZn(0.02), (b) recovered Pd/NiZn(0.02), (c) fresh Pd/HT(0.02), (d) recovered Pd/HT(0.02), (e) fresh Pd/NiZn(1), and (f) recovered Pd/NiZn(1).

to be coordinated to the monomeric Pd²⁺ center. The distances from the Pd atoms to the nearest oxygen atoms were essentially consistent with the values determined by X-ray crystallography for the Pd–O bond ($r = 2.02 \text{ \AA}$) in Pd oxide. Based on the above results, we propose that the local structure of the Pd species in the NiZn interlayer is a monomeric divalent hydroxyl complex, as shown in Fig 7.

We explored the potential catalytic abilities of various clay–Pd nanocomposites for the oxidation of benzyl alcohols

Table 2 Curve-fitting analysis of EXAFS data for clay–Pd nanocomposite catalysts^a

Sample	Shell	C.N. ^b	r (Å) ^c	σ (Å) ^d
fresh Pd/NiZn(0.02)	Pd–O	4.1	2.01	0.048
recovered Pd/NiZn(0.02)	Pd–O	3.8	2.01	0.033
fresh Pd/HT(0.02)	Pd–O	4.8	1.99	0.058
recovered Pd/HT(0.02)	Pd–Pd ^e	4.5	2.82	0.081
fresh Pd/NiZn(1)	Pd–O	4.4	2.02	0.054
recovered Pd/NiZn(1)	Pd–O	4.1	2.02	0.013

^a Curve-fitting analysis was performed in k -space with the inverse FT of the $1.16 \text{ \AA} < r < 1.96 \text{ \AA}$ range using PdO as a standard material.

^b Coordination number. ^c Bond distance. ^d Debye–Waller factor. ^e Inverse FT of the $1.90 \text{ \AA} < r < 2.95 \text{ \AA}$ range was curve fitted in k -space using Pd foil as a standard.

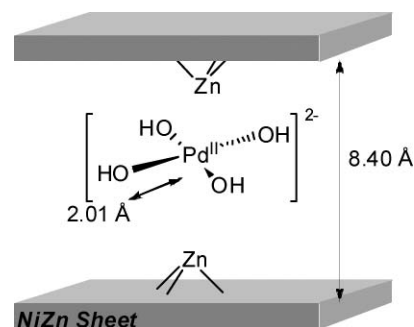


Fig. 7 Proposed structure around Pd(II) center of the Pd/NiZn(0.02) catalyst. The nearest oxygen atoms around the Pd(II) are shown.

under various conditions (Table 3). The Pd/NiZn(0.02) showed almost the same catalytic activity for benzyl alcohol oxidation under an air atmosphere as in a pure O₂ atmosphere, giving only benzaldehyde in an almost quantitative yield within 1 h (entries 1 and 2).¹⁰ Under a N₂ atmosphere, a small amount of benzaldehyde was formed, presumably due to the presence of residual O₂ (entry 3). The consumption of O₂ gas was measured, and an *ca.* 1:2 ratio of the O₂ uptake to benzaldehyde yield was observed, thereby suggesting that molecular oxygen was quantitatively used as the oxidant in the oxidative dehydrogenation. Furthermore, the control reaction of NiZn without any incorporated Pd species showed no activity toward alcohol oxidation, indicating that the Pd species was required for catalysis. In the case of the Pd/NiZn(1) catalyst, the rate of oxidation decreased due to the mass transfer limitation in

Table 3 Benzyl alcohol oxidation under various conditions^a

Entry	Catalyst	Conv _n (%) ^b	Yield (%) ^b
1	Pd/NiZn(0.02)	>99	97
2 ^c	Pd/NiZn(0.02)	>99	99
3 ^d	Pd/NiZn(0.02)	4	2
4	Pd/HT(0.02)	>99	>99
5	Pd/NiZn(1)	7	6
6 ^e	Pd/NiZn(0.02)	98	94
7 ^f	Pd/NiZn(0.02)	>99	94
8 ^g	NiZn	0	0
9	none	0	0

^a Benzyl alcohol (0.5 mmol), Pd catalyst (Pd: 2 mol%), PhCF₃ (2.5 mL), 353 K, 1 h, air flow (20 mL/min). ^b Determined by GC analysis using an internal standard technique. ^c Under 1 atm of O₂. ^d Under 1 atm of N₂. ^e 1st recycle. ^f 2nd recycle. ^g NiZn (0.5 g) was used as a catalyst.

the narrow interlayer space (entry 5). The use of HT as a catalyst support was tested with Pd/HT(0.02) and also resulted in excellent yields (entry 4), but the catalyst colour changed to dark brown (Fig. 8). From the Pd K-edge XANES and FT of the k^3 -weighted Pd K-edge EXAFS data for the recovered Pd/HT(0.02) catalyst, it was observed that Pd metal species were formed (Fig. 5d and 6d). The spent Pd/NiZn(0.02) catalyst was easily separated after the oxidation reaction by either simple centrifugation or filtration. The catalyst was found to be reusable without any reduction in activity (Table 3, entries 6 and 7). In order to further demonstrate the requirement of the Pd/NiZn(0.02) catalyst, the catalyst was removed by filtration when a test reaction reached 50% conversion. After removal of the catalyst, the reaction was monitored for an additional hour, and no additional product formation was observed. These results show that this reaction proceeds on the NiZn interlayer and any dissolved Pd species are not involved. It should be noted that no spectral change was observed in the Pd K-edge XANES, FT of k^3 -weighted Pd K-edge EXAFS spectra, or the curve-fitting analysis between fresh Pd/NiZn and recovered Pd/NiZn even in the case of the high Pd loading content in Pd/NiZn(1). This stability suggests that the Pd species remained in the divalent monomeric state throughout the course of the reaction. It can be said that the active divalent Pd species are created by strong electrostatic interactions between the anionic $[\text{Pd}(\text{OH})_4]^{2-}$ species and the layered NiZn host. To the best of our knowledge, this is the first demonstration of the formation of highly stable monomeric Pd species even at high Pd loading. The positive charge of HT is dispersed all over the brucite-type sheet, therefore the electrostatic interaction between HT host and intercalated-anions may become weaker than that of NiZn.

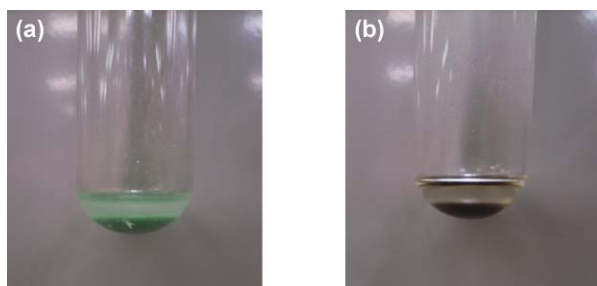


Fig. 8 Photoimages for (a) Pd/NiZn(0.02) and (b) Pd/HT(0.02) after the aerobic oxidation of benzyl alcohol. Reaction conditions were as follows: benzyl alcohol (0.5 mmol), Pd catalyst (Pd: 2 mol%), PhCF_3 (2.5 mL), 353 K, 1 h, air flow (10 mL/min).

The scope of the present Pd/NiZn(0.02) catalyst system toward oxidation of various alcohols was examined, and the results are summarized in Table 4. Primary benzylic alcohols with electron-donating substituents, such as *p*-methyl and *p*-methoxybenzyl alcohol, were converted to *p*-tolualdehyde and *p*-anisaldehyde in excellent yield, respectively (entries 2 and 3). On the other hand, the reaction rate of *p*-chlorobenzyl alcohol oxidation slightly decreased (entry 4). Moreover, the Pd/NiZn(0.02) catalyst showed a high turnover frequency (TOF; mol of product per mol of Pd content per hour) of 150 h^{-1} under an air atmosphere, as highlighted in entry 1. In the case of primary alcohol oxidation, the aldehydes were selectively obtained, and over-oxidation of the aldehyde

product to the corresponding carboxylic acid was not observed. The oxidation of secondary benzylic alcohols is also viable and affords the ketone products at a high yield (entries 5–7). In order to test for the possibility of a radical mechanism, the radical clock cyclopropyl phenyl carbinol was used as a substrate. Exclusive oxidation of the hydroxyl group, leading to the formation of the ketone product, was observed without any skeletal isomerization or carbon–carbon bond cleavage (entry 7). The Pd/NiZn(0.02) catalyst system was applicable to oxidation of allylic alcohols, nonactivated aliphatic alcohols, and cyclic aliphatic alcohols (entries 8–12). A primary aliphatic alcohol, 1-octanol, was successfully oxidized, affording 1-octanal without any formation of the corresponding carboxylic acid and ester (entry 10). Unfortunately, heterocyclic alcohols such as 2-pyridinemethanol and 2-thiophenemethanol were not oxidized to the corresponding carbonyl compounds with the Pd/NiZn(0.02) catalyst. The addition of radical scavengers, such as 2,2',6,6'-tetramethylpiperidine *N*-oxyl (TEMPO) or 2,6-di-*tert*-butyl-*p*-cresol, had little influence on the oxidation rate. This result, in combination with the radical clock studies, suggests that the catalytic system did not contain free radical intermediates. Notably, the oxidation of primary hydroxyl groups was selective even in the presence of secondary hydroxyl groups. For instance, an intramolecular competition experiment was carried out using 4-(1'-hydroxyethyl)benzyl alcohol. After 35% substrate consumption, 4-(1'-hydroxyethyl)benzaldehyde, 4-acetylbenzyl alcohol, and 4-acetylbenzaldehyde were observed at 29%, 1%, and 5% yields, respectively. This result shows that the rate of oxidation of primary alcohols is faster than that of secondary alcohols and suggests the formation of a Pd-alcoholate as an intermediate.¹¹ Competitive oxidations of *para*-substituted benzyl alcohols gave a Hammett ρ value of -0.148 ($R^2 = 0.94$), β -hydride elimination to form the carbocation-type intermediate is involved in the oxidation mechanism. From the above results, a plausible reaction mechanism for this alcohol oxidation in the NiZn interlayer was as follows: initially, the catalytic cycle begins with binding of the alcohol to the Pd(II) hydroxide species to form a Pd(II)-alkoxide species and H_2O . Following a β -hydride elimination, a Pd(II)-hydride species and the carbonyl product are formed. Then, the Pd(II)-hydride can reductively eliminate an equivalent of H_2O to form Pd(0), which is then reoxidized by molecular oxygen to form Pd-peroxide species. According to the Arrhenius plots of the reaction (323 K to 353 K, Fig. 9), the obtained activation energy (E_a) was 81.3 kJ mol^{-1} ($\ln A = 23.8$). The kinetic isotope effect for the intramolecular competitive oxidation of α -deuterio-*p*-methylbenzyl alcohol gave a $k_{\text{H}}/k_{\text{D}}$ value of 2.30 at 353 K in toluene- d_8 , which is consistent with kinetic isotope effects obtained for similar systems.^{3f,12} This implies that the elimination of β -hydride from the Pd-alcoholate species may be the rate-determining step.

Conclusions

We have synthesized a new NiZn–Pd nanocomposite catalyst containing highly stable divalent Pd species. The intercalated anionic Pd hydroxide complex was rigidly fixed by the strong electrostatic interactions characteristic of NiZn. Pd/NiZn(0.02) can act as an efficient heterogeneous catalyst for the oxidation of alcohols under an air atmosphere, without the need for any

Table 4 Aerobic alcohol oxidation catalyzed by Pd/NiZn(0.02) under 1 atm of air^a

Entry	Alcohol	Time (h)	Product	Convsn (%) ^b	Yield (%) ^b
1 ^c	R ¹ = H, R ² = H	2	R ¹ = H, R ² = H	90	90
2	R ¹ = Me, R ² = H	0.5	R ¹ = Me, R ² = H	>99	>99
3	R ¹ = OMe, R ² = H	0.5	R ¹ = OMe, R ² = H	>99	>99
4	R ¹ = Cl, R ² = H	7	R ¹ = Cl, R ² = H	16	11
5	R ¹ = H, R ² = Me	1	R ¹ = H, R ² = Me	>99	>99
6	R ¹ = H, R ² = Ph	12	R ¹ = H, R ² = Ph	92	90
7	R ¹ = H, R ² = cyclopropyl	10	R ¹ = H, R ² = cyclopropyl	85	81
8		2		>99	72
9		10		63	59
10 ^d		24		>99	>99
11 ^d		24		98	98
12 ^d		12		90	85
13 ^d		12		98	97
14 ^d		24		54	52
15 ^d		12		>99	96

^a Reaction conditions: alcohol (0.5 mmol), Pd/NiZn(0.02) (Pd: 2 mol%), PhCF₃ (2.5 mL), air flow (1 atm, 20 mL/min), 353 K. ^b Determined by GC analysis using an internal standard technique. ^c Benzyl alcohol (1 mmol), Pd/NiZn(0.02) (Pd: 0.3 mol%). ^d Reaction was carried out at 373 K.

additives. The features of the present NiZn-based catalysts, such as their (i) facile preparation and monomeric structure, (ii) easy recovery, and (iii) simple recycling are particularly desirable for “green” industrial organic transformations.

Experimental

General

All chemical compounds were purified by standard procedures¹³ before use. Analytical GLC was performed by a Shimadzu GC-8A with a flame ionization detector equipped with Silicone OV-17 and Silicone OV-101 packing. GC-MS was performed by a Shimadzu GC-17B with a thermal conductivity detector

equipped with an RT-βDEXsm capillary column. ¹H and ¹³C NMR spectra were obtained on JNM-AL400 or spectrometers at 400 MHz in chloroform-*d*₁ with TMS as an internal standard. Products were confirmed by the comparison of their GC retention time, mass, ¹H and ¹³C NMR spectra with those of authentic samples. Pd K-edge X-ray absorption fine structure spectra were recorded at room temperature in transmission and fluorescence modes using a Lytle detector with a Si(311) double crystal monochromator at the beam line NW-10A station with 6.5 GeV storage ring energy of the Photon Factory, AR, Tsukuba, Japan. (KEK-PF, proposal No. 2007G662). The resulting EXAFS spectra were analyzed with REX2000 (Rigaku Co.). Fourier transforms of *k*³-weighted EXAFS spectra were performed in the 3.5 Å⁻¹ < *k* < 13.0 Å⁻¹ range.

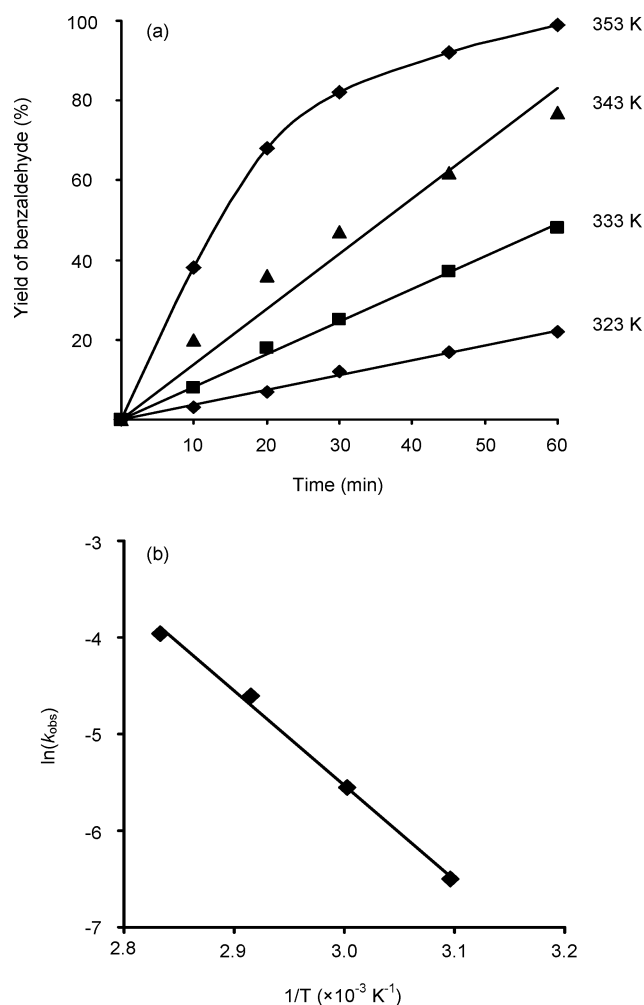


Fig. 9 (a) Effect of reaction temperature on the oxidation of benzyl alcohol. Reaction conditions: benzyl alcohol (0.5 mmol), Pd/NiZn(0.02) catalyst (Pd: 2 mol%), PhCF_3 (2.5 mL) and (b) Arrhenius plots for the oxidation of benzyl alcohol. Line fit: $\ln(k_{\text{obs}}) = 23.811 - 9.78/T$ ($r^2 = 0.996$).

Preparation of Ni–Zn mixed basic salt (NiZn)

Ni–Zn mixed basic salt (NiZn) was prepared according to literature procedures.^{7a} $\text{Ni}(\text{OAc})_2 \cdot 4\text{H}_2\text{O}$ (134 mmol) and $\text{Zn}(\text{OAc})_2 \cdot 2\text{H}_2\text{O}$ (66 mmol) were dissolved in deionized water (200 mL). The solution was hydrolyzed by heating in a TeflonTM-linked pressure bottle at 423 K for 24 h. The resulting precipitates were filtered, washed with deionized water, and dried under vacuum, yielding *ca.* 5 g of NiZn as a light green powder. From the XRF and TG-DTA analysis data, the compositional formula was derived as $\text{Ni}_{0.78}\text{Zn}_{0.44}(\text{OH})_2(\text{OAc})_{0.44} \cdot 0.86\text{H}_2\text{O}$.

Preparation of NiZn-supported Pd(II) catalyst (Pd/NiZn)

Pd/NiZn catalyst was prepared by a simple intercalation technique. K_2PdCl_4 (0.02 mmol, 6.50 mg) was dissolved in deionized water (40 mL), and 0.1 M NaOH (10 mL) was added, adjusted to pH 12.6. NiZn (1.0 g) was added to the resulting solution and stirred at room temperature for 3 h. The obtained slurry was filtered, washed with deionized water, and dried under

vacuum overnight, yielding Pd/NiZn(0.02) (0.99 g) as a light green powder.

General procedures for the aerobic benzyl alcohol oxidation using Pd/NiZn catalyst

Into a Schlenk tube with a reflux condenser was placed benzyl alcohol (0.5 mmol, 0.054 g), *n*-tetradecane (internal standard; 0.5 mmol, 0.0691 g), Pd/NiZn(0.02) (Pd: 2 mol%), and trifluorotoluene (2.5 mL). The resulting mixture was stirred at 353 K for 1 h under air flow conditions (20 mL/min). Benzyl alcohol conversion and benzaldehyde yields were periodically determined by GC analysis using *n*-tetradecane as an internal standard.

Procedure for reuse experiment

The first run of the aerobic oxidation of benzyl alcohol catalyzed by Pd/NiZn(0.02) was performed by the above described procedure. After catalytic reaction, Pd/NiZn(0.02) catalyst was separated by centrifugation. Separated Pd/NiZn(0.02) was washed with acetone (20 mL \times 4) and dried under vacuum at room temperature before recycling for the next run.

Oxygen uptake measurement

The uptake of molecular oxygen was measured by the following experiment. Pd/NiZn(0.02) catalyst (Pd: 2 mol%) was placed in a side-armed flask with a reflux condenser attached to a gas burette. The system was evacuated and filled with molecular oxygen, followed by the addition of trifluorotoluene (2.5 mL) and benzyl alcohol (0.5 mmol, 0.054 g), and then reacted for 1 h at 353 K. The molar ratio of O_2 gas uptake to benzaldehyde was *ca.* 1:2.

Synthesis of 4-(1'-hydroxyethyl)benzyl alcohol^{11b}

4-(1'-Hydroxyethyl)benzyl alcohol was synthesized by the reduction of 4-acetylbenzoic acid using lithium aluminium hydride (LiAlH_4) according to literature procedures. A solution of 4-acetylbenzoic acid (5 g, 34.5 mmol) in dry THF (20 mL) was added slowly to a suspension of LiAlH_4 (4 g, 132 mmol) in dry THF (30 mL) at room temperature, and the resulting mixture was refluxed overnight under a N_2 atmosphere. The mixture was cooled to room temperature and unreacted LiAlH_4 was destroyed by the addition of water, and an aqueous solution of NaOH (50 mL, 0.1 M) was added slowly to the mixture. The resulting solid was removed by filtration and washed with THF. The combined filtrate was dried and evaporated to give 4-(1'-hydroxyethyl)benzyl alcohol as a white powder.

Synthesis of α -deuterio-*p*-methylbenzyl alcohol^{11d}

α -Deuterio-*p*-methylbenzyl alcohol was synthesized by the reduction of *p*-methylbenzaldehyde using lithium aluminium deuteride (LiAlD_4) by a modification of the procedure reported for the synthesis of deuterium-labeled toluene. A solution of *p*-methylbenzaldehyde (3.2 g, 26.7 mmol) in dry THF (20 mL) was added slowly to a suspension of LiAlD_4 (0.33 g, 7.9 mmol) in dry THF (20 mL) at room temperature, and the resulting mixture was refluxed under N_2 atmosphere for 8 h. The mixture

was cooled to room temperature and unreacted LiAlD₄ was destroyed by the addition of water, and an aqueous solution of NaOH (50 mL, 0.1 M) was added slowly to the mixture. The resulting solid was removed by filtration and washed with THF. The combined filtrate was dried and evaporated to give α -deuterio-*p*-methylbenzyl alcohol as a white powder.

Intramolecular competitive aerobic oxidation of 4-(1'-hydroxyethyl)benzyl alcohol

The intramolecular competitive aerobic oxidation of 4-(1'-hydroxyethyl)benzyl alcohol was carried out under standard conditions. The reaction mixture was analyzed by GC and the products were identified by GC-MS and were identical to the literature values.

4-(Hydroxymethyl)acetophenone: m/z 150 (M⁺, 31), 135 (100), 107 (23), 89 (37), 77 (29).

4-(1'-Hydroxyethyl)benzaldehyde: m/z 150 (M⁺, 5), 149 (5), 107 (100), 79 (74), 77 (50), 51 (21).

4-Acetylbenzaldehyde: m/z 148 (M⁺, 41), 134 (17), 133 (100), 105 (49), 77 (33), 51 (24), 50 (15).

Kinetic isotope effect for the competitive aerobic oxidation of α -deuterio-*p*-methylbenzyl alcohol

α -Deuterio-*p*-methylbenzyl alcohol (0.5 mmol) and Pd/NiZn (0.5 g, Pd: 2 mol%) were dissolved in toluene-*d*₈ (2.5 mL) at 353 K under an air flow. The reaction mixture was stirred for 0.5 h yielding 20% *p*-methylbenzaldehyde. The *p*-methylbenzaldehyde yield was determined by GC-MS analysis using biphenyl as an internal standard. The kinetic isotope effect value (k_H/k_D) was determined by ¹H-NMR estimating the ratio of α -deuterio-*p*-methylbenzaldehyde to *p*-methylbenzaldehyde yield.

Acknowledgements

This study was supported by a Grant-in-Aid for Scientific Research from the Ministry of Education, Culture, Sports, Science, and Technology of Japan (19760540 and 1956077). Some of the experiments were carried out at a facility in the Photon Factory (KEK-PF, Proposal No. 2007G662).

Notes and references

- (a) I. W. C. E. Arends, and R. A. Sheldon, in *Modern Oxidation Methods*, ed. J.-E. Bäckvall, Wiley-VCH, Weinheim, 2004, p. 83; (b) T. Mallat and A. Baiker, *Chem. Rev.*, 2004, **104**, 3037; (c) I. E. Markó, P. R. Giles, M. Tsukazaki, A. Gautier, R. Dumeunier, K. Doda, F. Philippart, I. Chellé-Regnault, J.-L. Mutonkole, S. M. Brown, and C. J. Urech, in *Transition Metals for Organic Synthesis*, Vol. 2 (Eds. M. Beller, C. Bolm), Wiley-VCH, Weinheim, Germany, 2004, pp. 437; (d) M. J. Schultz and M. S. Sigman, *Tetrahedron*, 2006, **62**, 8227; (e) T. Matsumoto, M. Ueno, N. Wang and S. Kobayashi, *Chem.-Asian J.*, 2008, **3**, 196.
- Supported transition metal catalyst, Ru:(a) C. Mondelli, D. Ferri and A. Baiker, *J. Catal.*, 2008, **258**, 170; (b) M. Kotani, T. Koike, K. Yamaguchi and N. Mizuno, *Green Chem.*, 2006, **8**, 735; (c) T. Matsumoto, M. Ueno, N. Wang and S. Kobayashi, *Chem.-Asian J.*, 2008, **3**, 239; (d) K. Mori, S. Kanai, T. Hara, T. Mizugaki, K. Ebitani, K. Jitsukawa and K. Kaneda, *Chem. Mater.*, 2007, **19**, 1249; (e) K. Ebitani, K. Motokura, T. Mizugaki and K. Kaneda, *Angew. Chem., Int. Ed.*, 2005, **44**, 3423; (f) K. Yamaguchi and N. Mizuno, *Angew. Chem., Int. Ed.*, 2002, **41**, 4538Au; (g) F.-Z. Su, Y.-M. Liu, L.-C. Wang, Y. Cao, H.-Y. He and K.-N. Fan, *Angew. Chem., Int. Ed.*, 2008, **47**, 334; (h) A. Abad, P. Concepción, A. Corma and H. García, *Angew. Chem., Int. Ed.*, 2005, **44**, 4066; (i) H. Miyamura, R. Matsubara, Y. Miyazaki and S. Kobayashi, *Angew. Chem., Int. Ed.*, 2007, **46**, 4151; (j) H. Tsunoyama, H. Sakurai, Y. Negishi and T. Tsukuda, *J. Am. Chem. Soc.*, 2005, **127**, 9374; (k) D. I. Enache, J. K. Edwards, P. Landon, B. Solsona-Espriu, A. F. Carley, A. A. Herzing, M. Watanabe, C. J. Kiely, D. W. Knight and G. J. Hutchings, *Science*, 2006, **311**, 362Pt; (l) Y. M. A. Yamada, T. Arakawa, H. Hocke and Y. Uozumi, *Angew. Chem., Int. Ed.*, 2007, **46**, 704; (m) H. Miyamura, M. Shiramizu, R. Matsubara and S. Kobayashi, *Angew. Chem., Int. Ed.*, 2008, **47**, 8093.
- (a) S. Samanta and A. K. Nandi, *J. Phys. Chem. C*, 2009, **113**, 4721; (b) E. V. Chubarova, M. H. Dickman, B. Keita, L. Nadjo, F. Miserque, M. Mifsud, I. W. C. E. Arends and U. Kortz, *Angew. Chem., Int. Ed.*, 2008, **47**, 9542; (c) K. Hara, S. Tayama, H. Kano, T. Masuda, S. Takakusagi, T. Kondo, K. Uosaki and M. Sawamura, *Chem. Commun.*, 2007, 4280; (d) A.-H. Lu, W.-C. Li, Z. Hou and F. Schüth, *Chem. Commun.*, 2007, 1038; (e) B. Karimi, S. Abedi, J. H. Clark and V. Budarin, *Angew. Chem., Int. Ed.*, 2006, **45**, 4776; (f) K. Mori, T. Hara, T. Mizugaki, K. Ebitani and K. Kaneda, *J. Am. Chem. Soc.*, 2004, **126**, 10657; (g) Y. Uozumi and R. Nakao, *Angew. Chem., Int. Ed.*, 2003, **42**, 194.
- Handbook of Organopalladium Chemistry for Organic Synthesis*, ed. E. Negishi, Vol. 1-2, John Wiley & Sons, Inc., New York, 2002.
- It has been reported that atomically dispersed Pd²⁺ species on meso-Al₂O₃ surface did not aggregate during aerobic alcohol oxidation only under ultra diluted Pd loading amount (0.03 wt%), see: S. F. J. Hackett, R. M. Brydson, M. H. Gass, I. Harvey, A. D. Newman, K. Wilson and A. F. Lee, *Angew. Chem., Int. Ed.*, 2007, **46**, 8593.
- (a) G. Poncelet, J. J. Fripiat, in *Handbook of Heterogeneous Catalysis, 2nd Edition* (Ed. G. Ertl) Wiley-VCH, Weinheim, 2008, 1, pp. 219; (b) C. Forano, T. Hibino, F. Leroux and C. Taviot-Gueho, *Dev. Clay Sci.*, 2006, **1**, 1021; (c) F. Figueras, M. L. Kantam and B. M. Choudary, *Curr. Org. Chem.*, 2006, **10**, 1627; (d) D. Tichit and B. Coq, *CATTECH*, 2003, **7**, 206; (e) G. Centi and S. Perathoner, *Microporous Mesoporous Mater.*, 2008, **107**, 3.
- (a) S. Yamanaka, K. Ando and M. Ohashi, *Mater. Res. Soc. Symp. Proc.*, 1995, **371**, 131; (b) E. Kandare and J. M. Hossenlopp, *Inorg. Chem.*, 2006, **45**, 3766; (c) H. Morioka, H. Tagaya, M. Karasu, J. Kadokawa and K. Chiba, *Inorg. Chem.*, 1999, **38**, 4211; (d) M. Meyn, K. Beneke and G. Lagaly, *Inorg. Chem.*, 1993, **32**, 1209; (e) R. Rojas, C. Barriga, M. A. Ulibarri, P. Malet and V. Rives, *J. Mater. Chem.*, 2002, **12**, 1071; (f) J.-H. Choy, Y.-M. Kwon, K.-S. Han, S.-W. Song and S. H. Chang, *Mater. Lett.*, 1998, **34**, 356.
- T. Harada, S. Ikeda, M. Miyazaki, T. Sakata, H. Mori and M. Matsumura, *J. Mol. Catal. A: Chem.*, 2007, **268**, 59.
- The treatment of NiZn with an aqueous NaOH solution lead to the reduction of C. S., confirmed by XRD profile. Moreover, the exchange of interlayer acetate anion to hydroxyl anion was able to detect by FT-IR spectra, see ESI†.
- Aerobic benzaldehyde oxidation using our Pd/NiZn catalyst was carried out, however, the formation of benzoic acid was not observed after 1 h, and benzaldehyde still remained in the reaction mixture. Reaction conditions were as follows: benzaldehyde (0.5 mmol), Pd/NiZn(0.02) catalyst (Pd: 2 mol%), PhCF₃ (2.5 mL), 353 K, and air flow (20 mL/min), and products were determined by GC analysis using an internal standard technique.
- (a) P. A. Shapley, N. Zhang, J. L. Allen, D. H. Pool and H.-C. Liang, *J. Am. Chem. Soc.*, 2000, **122**, 1079; (b) A. Dijkstra, A. Marino-González, A. M. I. Payeras, I. W. C. E. Arends and R. A. Sheldon, *J. Am. Chem. Soc.*, 2001, **123**, 6826; (c) K. Yamaguchi, K. Mori, T. Mizugaki, K. Ebitani and K. Kaneda, *J. Am. Chem. Soc.*, 2000, **122**, 7144; (d) K. Yamaguchi and N. Mizuno, *Chem.-Eur. J.*, 2003, **9**, 4353.
- (a) K. Zaw, M. Lautens and P. M. Henry, *Organometallics*, 1985, **4**, 1286; (b) B. A. Steinhoff, S. R. Fix and S. S. Stahl, *Org. Lett.*, 2002, **4**, 4179; (c) G.-J. ten Brink, I. W. C. E. Arends and R. A. Sheldon, *Adv. Synth. Catal.*, 2002, **344**, 355; (d) J. A. Mueller, D. R. Jensen and M. S. Sigman, *J. Am. Chem. Soc.*, 2002, **124**, 8202; (e) J. A. Mueller and M. S. Sigman, *J. Am. Chem. Soc.*, 2003, **125**, 7005.
- W. L. F. Armarego, and C. L. L. Chai, *Purification of Laboratory Chemicals*, Elsevier, 2003.